Supporting Information

Néel-type optical target skyrmions inherited from evanescent electromagnetic fields with rotational symmetry

Bo Tian,[a†] Jingyao Jiang,[a†] Zebo Zheng,[a] Ximiao Wang,[a] Shaojing Liu,[a] Wuchao Huang,[a] Tian Jiang,*[b] Huanjun Chen,*[a] and Shaozhi Deng[a]

Note S1:The definition of the angle φ between the vector of the Néel-type target skyrmion and 2D plane supporting the target skyrmion

The Néel-type target skyrmion in 3D space are shown in Fig. S1. It can be found that the angle φ between the vector of the Néel-type target skyrmion and 2D plane supporting the target skyrmion can be divided into four situations φ_1, φ_2, φ_3, and φ_4 (Fig. S1). For a simpler description, we specify that when the vector points toward the positive z direction, the angle φ is positive, while it is negative when the vector points toward the negative z direction. Therefore, in Fig. S1, the angles φ_1 and φ_4 are positive, while the angles φ_2 and φ_3 are negative. The angle at a specific point can be expressed as:

$$\phi = \begin{cases} \tan^{-1}\left(e_z / e_r\right), & e_r \geq 0 \\ -\tan^{-1}\left(e_z / e_r\right), & e_r < 0 \end{cases} \tag{S1}$$

where e_z and e_r are the z-component and in-plane component of the vector of the Néel-type target skyrmion, respetively.

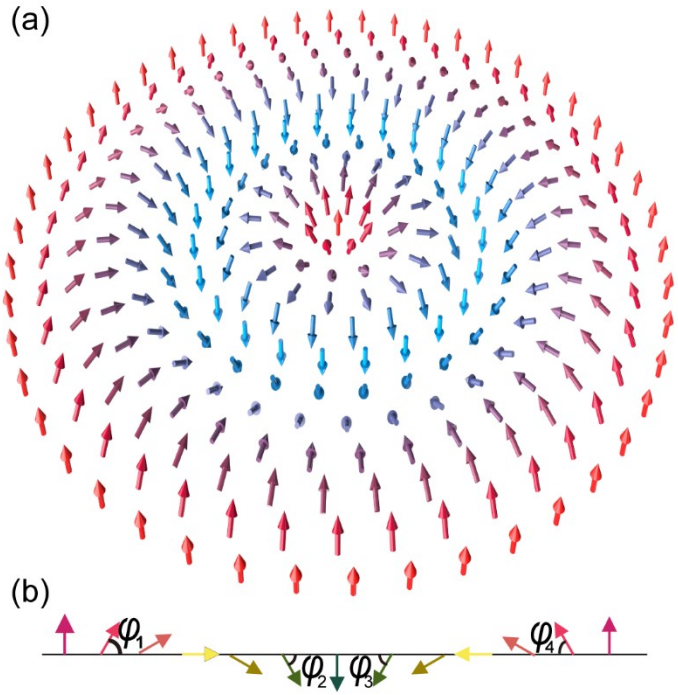

Fig. S1 Néel-type target skyrmion. (a) Distribution of the vector fields in a Néel-type target skyrmion with rotational symmetry. (b) Distribution of the vector fields along a specific radial direction, showing a cycling from the up state (φ = 90°) at the center of the target skyrmion to down state (φ = −90°) and then back to up state along the radial direction. The angle between the vector and the 2D plane where the target skyrmion is located can be divided into four situations as shown in (b).

Note S2:The skyrmion number of the target skyrmion with rotational symmetry

The topological invariant *S* of a target skyrmion is defined in Cartesian coordinate system as:

$$S = \frac{1}{4\pi}\iint_D \vec{e}\cdot\left(\partial_x \vec{e}\times\partial_x \vec{e}\right)dxdy \tag{S2}$$

where *D* is the integration area, $\vec{e}$ is the normalized three-dimensional vector. When the angular component of the $\vec{e}$ in the cylindrical coordinate system (r, θ, z) is 0, the vector $\vec{e}$ can be expressed as:

$$\vec{e} = \cos\varphi\hat{i}_r + \sin\varphi\hat{i}_z \tag{S3}$$

Where φ is a function of the coordinates *r*, indicating the angle between the vector $\vec{e}$ and the plane where *D* is located. Because the relationships between the unit direction vector $\hat{i}_r$ and $\hat{i}_\theta$ in the cylindrical coordinate system and the unit vector $\hat{i}_x$ and $\hat{i}_y$ in the Cartesian coordinate system are

$$\hat{i}_r = \frac{x}{\sqrt{x^2+y^2}}\hat{i}_x + \frac{y}{\sqrt{x^2+y^2}}\hat{i}_y \tag{S4a}$$

$$\hat{i}_\theta = \frac{-y}{\sqrt{x^2+y^2}}\hat{i}_x + \frac{x}{\sqrt{x^2+y^2}}\hat{i}_y \tag{S4b}$$

Therefore, the derivative of the unit direction vector $\hat{i}_r$ and $\hat{i}_\theta$ with respect to the independent variables *x* and *y* are

$$\frac{\partial\hat{i}_r}{\partial x} = \frac{y^2}{r^3}\hat{i}_x - \frac{xy}{r^3}\hat{i}_y = -\frac{y}{r^2}\hat{i}_\theta \tag{S5a}$$

$$\frac{\partial\hat{i}_r}{\partial y} = -\frac{xy}{r^3}\hat{i}_x + \frac{x^2}{r^3}\hat{i}_y = \frac{x}{r^2}\hat{i}_\theta \tag{S5b}$$

Then the derivative of the normalized unit vector $\vec{e}$ defined in Eq. (S3) with respect to the independent variable *x* and *y* are

$$\frac{\partial\vec{e}}{\partial x} = \cos\varphi\frac{\partial\varphi}{\partial x}\hat{i}_z - \sin\varphi\frac{\partial\varphi}{\partial x}\hat{i}_r - \frac{y}{r^2}\cos\varphi\hat{i}_\theta \tag{S6a}$$

$$\frac{\partial\vec{e}}{\partial y} = \cos\varphi\frac{\partial\varphi}{\partial y}\hat{i}_z - \sin\varphi\frac{\partial\varphi}{\partial y}\hat{i}_r + \frac{x}{r^2}\cos\varphi\hat{i}_\theta \tag{S6b}$$

Then the form of the integrand in Eq. (S2) can be expressed as

$$\vec{e}\cdot\left(\frac{\partial\vec{e}}{\partial x}\times\frac{\partial\vec{e}}{\partial y}\right) = -\frac{\cos\varphi}{r^2}\left(y\frac{\partial\varphi}{\partial y} + x\frac{\partial\varphi}{\partial x}\right) = -\frac{\cos\varphi}{r}\frac{\partial\varphi}{\partial r} \tag{S7}$$

Therefore, for the vector distribution as shown in Eq. (S3), the topological invariance of target skyrmion can be transformed as

$$S = -\frac{1}{4\pi}\iint_D \frac{\cos\varphi}{r}\frac{\partial\varphi}{\partial r}rdrd\theta = -\frac{1}{2}\int_D \cos\varphi\frac{\partial\varphi}{\partial r}dr \tag{S8}$$

According to Eq. (S8), *S* is always equal to 1 (0) as long as the angle φ changes from π/2 to −π/2 (π/2).

Note S3: The relationship between the different components of electric fields of TM electromagnetic waves in a cylindrical coordinate system

When both the current density and charge density are zero, Maxwell's equations can be expressed as:

$$\nabla \times \vec{E} = \frac{1}{r}\begin{bmatrix} \vec{e}_r & r\vec{e}_\theta & \vec{e}_z \\ \frac{\partial}{\partial r} & \frac{\partial}{\partial \theta} & \frac{\partial}{\partial z} \\ E_r & rE_\theta & E_z \end{bmatrix} = i\omega\mu_0 \vec{H} \tag{S9}$$

and:

$$\nabla \times \vec{H} = \frac{1}{r}\begin{bmatrix} \vec{e}_r & r\vec{e}_\theta & \vec{e}_z \\ \frac{\partial}{\partial r} & \frac{\partial}{\partial \theta} & \frac{\partial}{\partial z} \\ H_r & rH_\theta & H_z \end{bmatrix} = -i\omega\varepsilon_0 \vec{E} \tag{S10}$$

By expanding Eq. (S9) and (S10), one can lead to the following relations between different components of the electric field and magnetic field strengths:

$$\frac{1}{r}\frac{\partial E_z}{\partial \theta} - \frac{\partial E_\theta}{\partial z} = i\omega\mu_0 H_r \tag{S11a}$$

$$\frac{\partial E_r}{\partial z} - \frac{\partial E_z}{\partial r} = i\omega\mu_0 H_\theta \tag{S11b}$$

$$\frac{1}{r}\frac{\partial (rE_\theta)}{\partial r} - \frac{1}{r}\frac{\partial E_r}{\partial \theta} = i\omega\mu_0 H_z \tag{S11c}$$

and:

$$\frac{1}{r}\frac{\partial H_z}{\partial \theta} - \frac{\partial H_\theta}{\partial z} = -i\omega\varepsilon_0 E_r \tag{S12a}$$

$$\frac{\partial H_r}{\partial z} - \frac{\partial H_z}{\partial r} = -i\omega\varepsilon_0 E_\theta \tag{S12b}$$

$$\frac{1}{r}\frac{\partial (rH_\theta)}{\partial r} - \frac{1}{r}\frac{\partial H_r}{\partial \theta} = -i\omega\varepsilon_0 E_z \tag{S12c}$$

For a TM ($H_z = 0$) electromagnetic waves, the dependence of the electric field on the coordinate z and t is $\exp(ik_z' z - i\omega t)$. By plugging Eq. (S12a) into (S11b), one can obtain:

$$E_r = \frac{ik_z'}{k_s^2}\frac{\partial E_z}{\partial r} \tag{S13}$$

By plugging the Eq. (S12b) to (S11a), one can obtain:

$$E_\theta = \frac{ik_z'}{rk_s^2}\frac{\partial E_z}{\partial \theta} \tag{S14}$$

where k_s is the in-plane wave vector, and satisfies $k_s^2 + k_z'^2 = k_0^2$. $k_0 = \omega\sqrt{\mu_0\varepsilon_0}$ is the wave vector in vacuum. When $k_z' = ik_z$ is an imaginary number, the electric field is an evanescent wave in the z-direction and the dependence of the electric field on the coordinate z is $\exp(-k_z z)$. Eq. (S13) and (S14) then become:

$$\begin{cases} E_r = -\dfrac{k_z}{k_s^2}\dfrac{\partial E_z}{\partial r} \\ E_\theta = -\dfrac{k_z}{rk_s^2}\dfrac{\partial E_z}{\partial \theta} \end{cases} \tag{S15}$$

where the wave vector satisfies $k_s^2 - k_z^2 = k_0^2$.

Note S4: Fourier transform of rotationally symmetric functions

The Fourier transform (FT) of a binary functions $f(x,y)$ is defined as:

$$F\left(k_x, k_y\right)=\frac{1}{2\pi}\int_{-\infty}^{\infty}\int_{-\infty}^{\infty} f(x,y)e^{-i(k_x x+k_y y)}dxdy \tag{S16}$$

where (x, y) and (k_x, k_y) are the independent variables in real space and momentum space, respectively. The relations between the different variables in Cartesian coordinate system and polar coordinate system are:

$$x=r\cos\theta, y=r\sin\theta, k_x=\rho\cos\beta, k_y=\rho\sin\beta \tag{S17}$$

where r and ρ are the independent polar variables in real space and momentum space, respectively. Therefore, the FT (S16) can be expressed as:

$$F(\rho\cos\beta,\rho\sin\beta)=\frac{1}{2\pi}\int_0^{2\pi}\int_0^{\infty} f(r\cos\theta,r\sin\theta)e^{-i\rho r\cos(\theta-\beta)}rdrd\theta \tag{S18}$$

When the function f is independent on θ, Eq. (S18) can be expressed as:

$$F(\rho\cos\beta,\rho\sin\beta)=\frac{1}{2\pi}\int_0^{2\pi}\int_0^{\infty} f(r)e^{-i\rho r\cos(\theta-\beta)}rdrd\theta \tag{S19}$$

Due to the existence of definite integral:

$$\int_0^{2\pi} e^{-i\rho r\cos(\theta-\beta)}d\theta=2\pi J_0(\rho r) \tag{S20}$$

Eq. (S19) can be simplified as:

$$F(\rho\cos\beta,\rho\sin\beta)=\int_0^{\infty} rf(r)J_0(\rho r)dr \tag{S21}$$

Because the right-hand side of the Eq. (S21) is not a function of β, the left-hand side of the equation should not be a function of angle β either. Therefore, Eq. (S21) can be expressed as:

$$F\left(\rho\right)=\int_0^{\infty} rf(r)J_0(\rho r)dr \tag{S22}$$

Similarly, the expressions of the inverse FT is:

$$f\left(r\right)=\int_0^{\infty}\rho F(\rho)J_0(\rho r)d\rho \tag{S23}$$

According to the above analysis, when a function f is rotationally symmetric, its FT F must be rotationally symmetric, and vice versa. Eq. (S22) and (S23) are 2D FT of rotationally symmetric functions, also known as the zero-order Hankel transform.

For the rotationally symmetric function $C\delta(\rho-k_s)$ illustrated in the lower left corner of Fig. 2(a), its inverse FT can be found by Eq. (S23). Then field intensity is:

$$E_z(r)=\int_0^{\infty}\rho C\delta\left(\rho-k_s\right)J_0\left(\rho r\right)d\rho=Ck_sJ_0\left(k_s r\right) \tag{S24}$$

Since the function decays exponentially in the z-direction, the entire distribution of the electric field intensity can be expressed as

$$E_z\left(r,z\right)=Ck_sJ_0(k_s r)e^{-k_z z} \tag{S25}$$

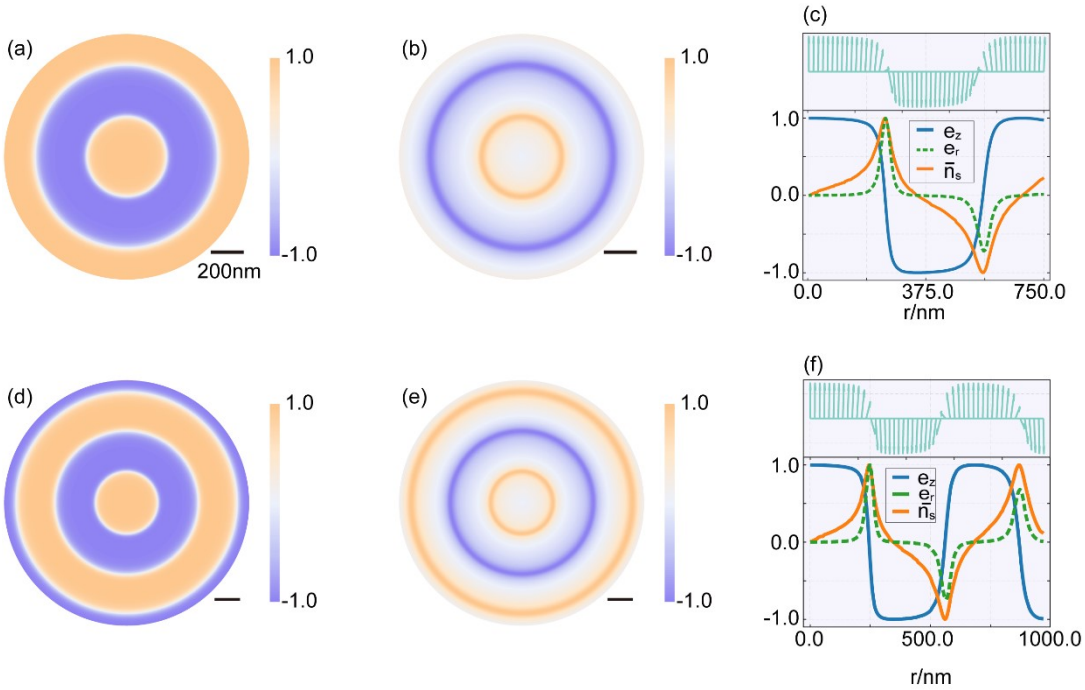

Fig. S2 Néel-type optical target skyrmions formed by surface plasmon polaritons in a gold flake. (a, b, d, e) Distributions of the normalized electric field component ez (a, d) and er (b, e) above the gold flake. (c, f) Radial variations of the ez, er, and along a specific in-plane direction. Upper panels in (c) and (f): radial evolvements of the electric field vector. A z-polarized electric dipole is employed as the excitation, which is placed 100 nm above the gold flake. The electric field signals were obtained on the plane 50 nm above the sample surface. The excitation wavelengths are 532 nm (a–c) and 633 nm (d–e), respectively. The thickness of the gold flake is 200 nm. Scale bars are 200 nm.

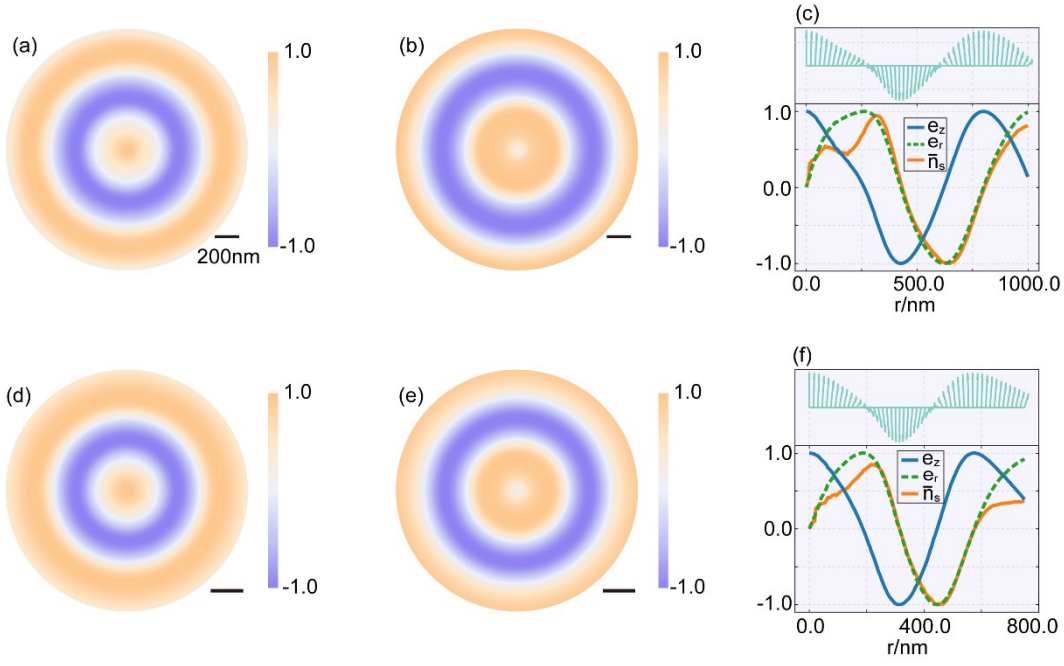

Fig. S3 Néel-type optical target skyrmions formed by phonon polaritons in an hBN flake. (a, b, d, e) Distributions of the normalized electric field component e_z (a, d) and e_r (b, e) above the gold flake. (c, f) Radial variations of the e_z, e_r, and $\overline{n}_s$ along a specific in-plane direction. Upper panels in (c) and (f): radial evolvements of the electric field vector. A *z*-polarized electric dipole is employed as the excitation, which is placed 100 nm above the hBN flake. The electric field signals were obtained on the plane 50 nm above the sample surface. The excitation wavelengths are 12.66 μm (a−c) and 12.50 μm (d−e), respectively. The thickness of the hBN flake is 200 nm. Scale bars are 200 nm.

Table S1 The coordinates of the zeros of e_r and $\overline{n}_s$, and the extreme points of e_z in Figs. 1−6 in the main text.

Radial coordinate	e_r	$\overline{n}_s$	e_z
Fig.1: $k_s r$	3.832	3.832	3.832
	7.016	7.016	7.016
	10.173	10.173	10.173
	13.324	13.324	13.324
Fig. 2: *r* (nm)	52	52	52
	98	98	98
Fig. 3: *r* (nm)	46	46	46
	88	88	88
Fig. 4(a-c):*r* (nm)	349	349	349
	687	687	687
Fig. 4(d-f): r (nm)	347	347	347
	683	683	683
Fig. 5(a-c): r (nm)	426	426	426
	800	800	800
Fig. 5(d-f): r (nm)	312	312	312
	571	571	571
Fig. 6: r (nm)	72	72	72
	146	146	146

Table S2. The values of the topological invariants.

	topological invariant S	
Fig. 2	0.995	−0.994
Fig. 3	0.993	−0.991
Fig. 4(a-c)	0.996	-1.003
Fig. 4(d-f)	1.005	-0.997
Fig. 5(a-c)	1.005	-0.994
Fig. 5(d-f)	0.993	-1.002
Fig. 6	1.007	−1.001